



Recent decrease in genesis productivity of tropical cloud clusters over the Western North Pacific

Haikun Zhao¹ · Shaohua Chen² · G. B. Raga³ · Philip J. Klotzbach⁴ · Liguang Wu⁵

Received: 2 May 2018 / Accepted: 30 September 2018
© Springer-Verlag GmbH Germany, part of Springer Nature 2018

Abstract

Tropical cloud clusters (TCCs) play a critical role in sustaining tropical large-scale systems and are traditionally viewed as precursors for tropical cyclone (TC) genesis. This study focuses on the decadal changes in genesis productivity (GP), e.g. the efficiency of TCCs developing into TCs, and shows a significant decrease in GP over the western North Pacific (WNP) basin since 1998, when a climate regime change occurred. The significant decrease in TC frequency and the significant increase in TCCs, especially over the eastern region of the WNP basin, have combined to result in a reduced GP since 1998. These changes are dependent on the combined changes in large-scale atmospheric-oceanic conditions over the WNP basin. A decadal change in vertical wind shear, especially over the eastern portion of the WNP basin, appears to be the most important contributor to the recent decrease in GP. Increased vertical wind shear suppresses TC genesis but enhances the frequency of TCCs. Secondary positive contributions to the recent decrease in GP are from local sea surface temperatures (SSTs) and low-level relative vorticity. These positive contributions to the recent decrease in GP are partly cancelled out by a negative contribution from enhanced mid-relative moisture. Changes in these large-scale conditions associated with the recent decrease in GP over the WNP basin since 1998 are closely related to the weakening monsoon circulation and the westward shift of the tropical upper-tropospheric trough over the WNP. This is likely related to the changes observed in tropical SST anomalies around the globe.

Keywords Tropical cloud cluster · Genesis productivity · Tropical cyclones · Western North Pacific · Pacific climate regime shift

1 Introduction

✉ Haikun Zhao
zhk2004y@gmail.com

¹ Key Laboratory of Meteorological Disaster, Ministry of Education(KLME)/Joint International Research Laboratory of Climate and Environment Change(ILCEC)/Collaborative Innovation Center on Forecast and Evaluation of Meteorological Disaster(CIC-FEMD)/Pacific Typhoon Research Center/Earth System Modeling Center, Nanjing University of Information Science and Technology, Nanjing 210044, China

² Key Laboratory of Meteorological Disaster of Ministry of Education, Nanjing University of Information Science and Technology, Nanjing, China

³ Centro de Ciencias de la Atmósfera, Universidad Nacional Autónoma de México, Mexico City, Mexico

⁴ Department of Atmospheric Science, Colorado State University, Fort Collins, CO, USA

⁵ Pacific Typhoon Research Center, Nanjing University of Information Science and Technology, Nanjing, China

Tropical cloud clusters (TCCs) are traditionally defined as synoptic-scale areas of deep convection and associated cirrus outflow composed of mesoscale convective systems. TCCs release large amounts of latent heat to sustain large-scale tropical systems and are generally viewed as necessary precursors for tropical cyclones (TCs) (McBride and Zehr 1981; Lee 1989; Hennon et al. 2011, 2013). Under favorable environmental conditions, a TCC can develop into a TC (Gray 1998). Enhanced understanding of the relationship between TCCs and TCs on various time scales, as well as the associated physical mechanisms, have important implications for both short-term predictions as well as long-term climate projections of TCs. This improved understanding consequently has the potential to mitigate societal impacts from TCs.

Large-scale atmospheric-oceanic environmental conditions are critical for the formation and development of

both TCCs and TCs (Williams and Houze 1987; Mapes and Houze 1993; Mohr and Zipser 1996; Chen et al. 1996; Gray 1998; Nesbitt et al. 2000; Kerns and Chen 2013; Hennon et al. 2011, 2013). For example, over the western North Pacific (WNP) basin, vigorous southeast–northwest-oriented wave trains along the monsoon trough favor TCCs. This monsoon trough is also a productive area for TC genesis (Holland 1995; Chen et al. 2008; Wu and Duan 2014; Wu et al. 2015a, b; Zhao et al. 2016). Generally, formation and development of TCs and TCCs share common large-scale environmental factors, such as large low-level relative vorticity, high mid-level relative humidity and warm sea surface temperatures (SSTs) (Gray 1968; McBride and Zehr 1981; Perrone and Lowe 1986; DeMaria et al. 2001; Hennon and Hobgood 2003; Hennon et al. 2005; Kerns and Zipser 2009; Fu et al. 2010; Peng et al. 2010). For example, McBride and Zehr (1981) found little difference in temperature and moisture between TCCs that developed into TCs and those that did not develop into TCs. Vertical wind shear was found to be one of the most important factors for discriminating developing systems from non-developing ones, with lower vertical wind shear tending to favor TCs but relatively larger vertical wind shear tending to favor TCCs (Zehr 1992; Gray 1998; Kerns and Zipser 2009; Kerns and Chen 2013).

Many studies have investigated the nature of TCCs and their associations with TCs on synoptic-to-mesoscale time-scales (Williams and Houze 1987; Mapes and Houze 1993; Chen et al. 1996; Mohr and Zipser 1996; Nesbitt et al. 2000; Kerns and Chen 2013). However, how the association between TCCs and TCs changes on longer time scales has been investigated much less frequently. One of the most important reasons is the lack of a long-period TCC dataset. Based upon the available new global, gridded satellite infrared (IR) dataset and the global TC best track dataset (International Best Track Archive for Climate Stewardship-IBTrACS; Knapp et al. 2010), Hennon et al. (2011) developed an objective tracking algorithm based upon the characteristics of atmospheric convection to identify global TCCs from 1982 to 2009. They also tracked the transition from TCCs into TCs. The longer-period global TCC dataset for the period from 1982 to 2009 provides a good chance to expand earlier efforts on synoptic-scale to mesoscale characterization by investigating inter-annual and inter-decadal variations of the association between TCCs and TCs. Hennon et al. (2013) conducted a follow-up study on the inter-annual and inter-decadal variability of both global and regional genesis productivity (GP). Teng et al. (2014) used Gridded Satellite (GridSat) data to track July–October TCCs over the western North Pacific (WNP) basin from 1981 to 2009 (as in Hennon et al. 2011) and further investigated the influence of El Niño–Southern Oscillation (ENSO) on TCCs and their GP. On the inter-decadal time scale, Hennon et al. (2013) pointed out a significant decrease in GP over the

WNP basin since 1998, but no detailed analysis of the recent significant decrease of GP over the WNP was conducted.

A significant reduction in TC frequency over the WNP basin since the late 1990s has been well documented in previous studies (Maue 2011; Liu and Chan 2013, Hsu et al. 2014; Zhao and Wang 2016, 2018; Hu et al. 2018; Zhao et al. 2018). These studies mainly attribute inter-decadal changes in the large-scale environment associated with the Pacific climate regime shift since 1998 to the recent decrease in TC counts over the WNP basin. Given the significant reduction in GP over the WNP basin since 1998 (Hennon et al. 2013), we pose the question: what has caused the reduction in GP over the WNP basin since the late 1990s? Also, what is the relative importance of large-scale factors in decreasing the GP during recent decades over the WNP basin?

The rest of this study is arranged as follows. Section 2 describes the datasets and the methodology used. Section 3 gives statistical analyses of changes in GP over the WNP basin prior to 1998 and since 1998. Section 4 investigates the changes in large-scale environmental factors as well as their relative importance. Section 4 also explores plausible physical explanations. A summary is given in Sect. 5.

2 Data and methods

2.1 TCC and TC datasets and definition of genesis productivity

We use global TCC data from the dataset described in Hennon et al. (2011, 2013). TCCs were objectively identified by GridSat-calibrated IR data with 8-km spatial resolution (Knapp et al. 2011) based on the characteristics of atmospheric convection, including size, shape, and persistence. Developing TCCs or those clusters that formed into a TC are identified by comparing their locations with the IBTrACS dataset (Knapp et al. 2010). Further details on the identification of TCCs and TCs can be found in Hennon et al. (2011, 2013). The TC formation location is defined as the latitude and longitude when a TC for the first time reached tropical storm intensity (17.2 m s^{-1}).

GP is used to measure the efficiency of TCCs developing into TCs, calculated as in Hennon et al. (2013), given by the following expression:

$$GP = \frac{TC(IBCAs)}{TCC(total)} \times 100\% \quad (1)$$

2.2 Large-scale atmospheric and oceanic datasets

Atmospheric fields were obtained from the NCEP-DOE (National Centers for Environmental Prediction-Department of Energy) AMIP-II monthly Reanalysis products

(Kanamitsu et al. 2002), which has a horizontal resolution of $2.5^{\circ} \times 2.5^{\circ}$ in longitude and latitude and 17 standard pressure levels. Vertical wind shear was calculated as the magnitude of the wind vector difference between 850hPa and 200hPa. The SST dataset used was the Extended Reconstructed SST version 3b (ERSST v3b) (Smith et al. 2008), which has a horizontal resolution of $2.0^{\circ} \times 2.0^{\circ}$ in longitude and latitude.

2.3 Diagnostic tool for the role of environmental factors

The Genesis Potential Index (GPI) from Emanuel and Nolan (2004) is adopted to diagnose the importance of the environmental factors controlling the recent decrease of GP over the WNP basin, and is given by the following expression:

$$GPI = \left| 10^5 \xi \right|^{3/2} \times \left(\frac{H}{50} \right)^3 \times \left(\frac{V_{pot}}{70} \right)^3 \times (1 + 0.1 \times V_{shear})^{-2} \quad (2)$$

where ξ represents the absolute vorticity (s^{-1}) at 850hPa, H represents the relative humidity (%) at 600hPa, and V_{pot} represents the potential intensity (PI) ($m s^{-1}$) that provides a theoretical upper bound on TC intensity under given specific environmental thermodynamic conditions. Details on the PI computation can be found in Bister and Emanuel (2002). V_{shear} is the vertical wind shear, computed as the magnitude of the vector difference between winds at 850hPa and 200hPa ($m s^{-1}$). The GPI was originally proposed to represent TC genesis potential by Emanuel and Nolan (2004). Studies have suggested that the GPI can capture the variability of TC genesis at various time scales including inter-decadal (Zhao et al. 2018, Hsu et al. 2014), inter-annual (Camargo et al. 2007; Tippett et al. 2011; Zhao and Raga 2014) and intra-seasonal (Camargo et al. 2009; Huang et al. 2011; Jiang et al. 2012; Zhao et al. 2015a, b, 2016, 2017, 2018; Zhao and Wu 2017). We show later that the GPI also successfully captures the recent decrease of GP over the WNP basin.

Following Camargo et al. (2007), and in order to further investigate the separate role of each of the four factors included in the GPI in determining the recent decrease in GP over the WNP basin, the GPI is calculated by varying one variable at a time and keeping the other three variables at their climatological values (1982–2009). These terms are referred to as GPI-RH, GPI-VOR, GPI-Shear, and GPI-PI, respectively, indicating the distinct contribution of mid-level relative humidity, low-level absolute vorticity, vertical wind shear and PI. The GPI with all four variables varying simultaneously is referred to as GPI-Total. Although the net anomaly cannot be described as the sum of the contributions from the four factors included in the GPI due to its nonlinearity, the index provides an adequate quantification of the role of each of the different factors. This methodology

has been adopted in a number of previous studies (Camargo et al. 2009; Huang et al. 2011; Jiang et al. 2012; Zhao et al. 2014, 2015a, b, 2018; Hu et al. 2018).

2.4 Statistical significance

The Student's *t* test was used to test statistical significance of the composite differences of all variables including large-scale oceanic and atmospheric fields. The Student's *t* test was also used to test for differences in correlations observed between the two time periods investigated here. All differences noted as significant in the remainder of the manuscript are significant at the 5% level.

3 Results of the GP statistical analysis

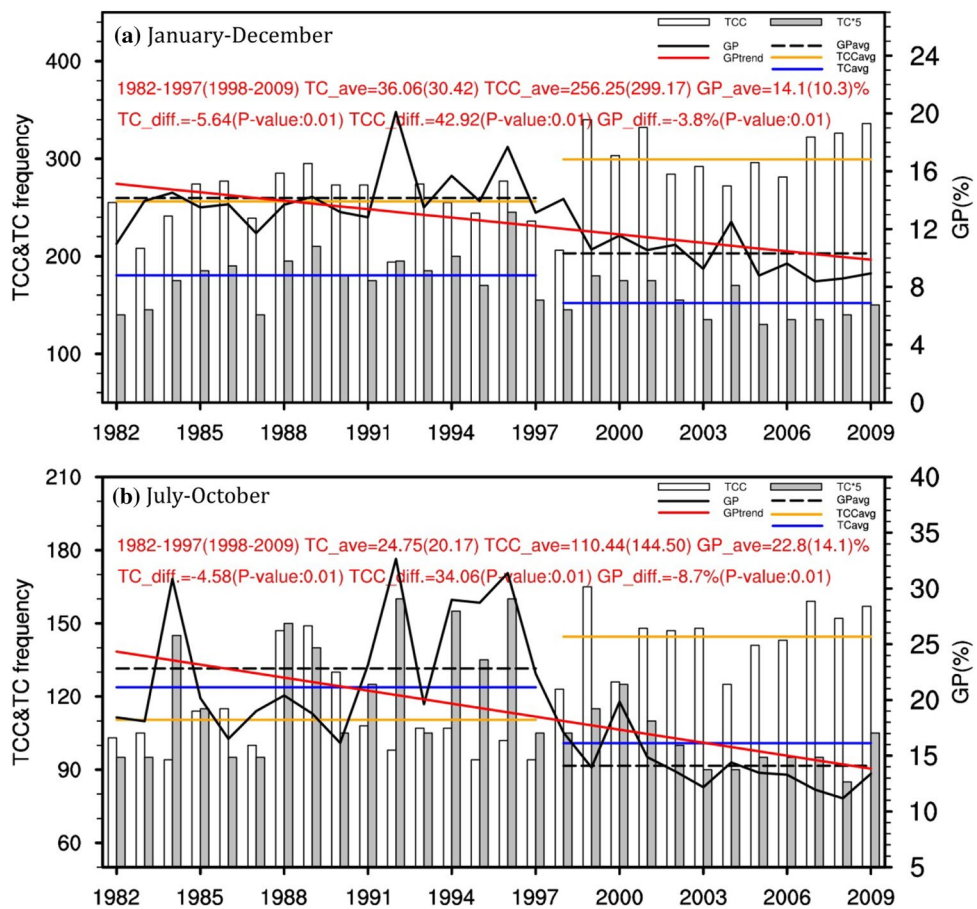
3.1 Linear trends and decadal variability

Annual GP (January–December) over the WNP basin shows a significant decreasing linear trend of -0.19% per year during 1982–2009 (Fig. 1a). The pronounced downward trend is directly related to the decadal changes of GP over the WNP basin. Coinciding with the Pacific climate regime shift around 1998, as suggested in previous studies (Zhao and Wang 2016, 2018; Hu et al. 2018), the GP over the WNP basin experienced a significant decrease from 1998 to 2009. Before 1998, the annual-averaged GP is 14.1%, which is significantly larger than the annual-averaged GP of 10.3% since 1998. These results are consistent with those reported by Hennon et al. (2013).

The significantly suppressed GP over the WNP basin since 1998 is found to be due to combined changes in both TCCs and TCs over the WNP basin during the recent period (Fig. 1a). The number of TCs over the WNP basin shows a significant decrease from 1998 to 2009 compared to the period from 1982 to 1997. The annual averaged TC count is 36 from 1982 to 1997, while the annual TC count is 30 from 1998 to 2009. In contrast, the number of TCCs experienced a significant increase during recent years compared to the average from 1982 to 1997. The average annual TCC count from 1982 to 1997 is 256 which increased significantly to 299 TCCs per year during 1998–2009.

Examination of the changes of GP over the WNP basin on seasonal timescales between the two sub-periods before 1998 and since 1998 suggests that the recent decrease in annual-averaged GP since 1998 is largely due to the significant decrease of boreal summer (July–October) GP (figure not shown). During the boreal summer, a significant downward trend of -0.39% per year is observed for GP during the full time period investigated from 1982 to 2009 (Fig. 1b). Note that the linear downward trend for GP during the boreal summer is larger than twice the annual linear (-0.39 vs.

Fig. 1 **a** Time series of the annual (i.e., January–December) western North Pacific (WNP) tropical cloud clusters (TCCs) (white bars), tropical cyclones (TCs) (grey bars; multiplied by 5), and genesis productivity (GP) (black solid line). The annual averaged TCs, TCCs and GP during 1982–1997 and 1998–2009 are indicated with a blue solid line, a yellow solid line, and a black dotted line, respectively. The linear trend in GP from 1982 to 2009 is indicated by the red solid line. **b** As in **a** except for the boreal summer from July to October



–0.19) trend over the WNP basin. Moreover, the significant decrease of GP during the boreal summer over the WNP basin since the late 1990s can be readily seen (Fig. 1b), with an average GP of 22.8% from 1982 to 1997 and an average GP of 14.1% from 1998 to 2009. Therefore, we mainly focus on the analyses of boreal summer GP and the associated possible explanations in the following sections, unless otherwise indicated.

3.2 Changes in the spatial distribution of GP

In addition to the observed change in GP over the WNP basin around 1998, there are also significant differences in the spatial distribution in GP. As shown in Fig. 2a, b, TCCs tend to concentrate in a region between 5°N–20°N, 100°E–180° during both sub-periods which coincides well with the main development region (MDR) for WNP TC activity. There is, however, a large difference in the frequency of occurrence with more TCCs observed since 1998. An obvious westward shift in TC genesis location over the WNP basin during recent decades has occurred, with a significant decrease in TCs over the eastern region of the WNP basin also occurring since 1998 (Fig. 2c).

Figure 2c also shows that TCCs have increased in a relatively spatially uniform manner, which is in pronounced contrast to the TC genesis shifts just discussed.

To further examine the changes of the spatial distribution of the GP, the whole WNP basin is divided into two sub-regions: (1) 0°–30°N, 100°E–140°E—the western portion of the WNP basin and (2) 0°–30°N, 140°E–180°—the eastern portion of the WNP basin. The recent decrease of GP over the WNP basin is mainly due to a sharp decrease in GP over the eastern portion of the WNP basin (Fig. 3). Over the eastern portion of the WNP basin, GP decreased from an average of 22.2% during 1982–1997 to 11.0% during 1998–2009 (Fig. 3). This result is a combination of significantly increased TCCs and significantly decreased TCs over this region in recent decades. In contrast, a small decrease of GP is observed over the western region of the WNP basin during recent decades, with a GP average of 19.6% during 1982–1997 and a GP average of 17.2% during 1998–2009 (Fig. 3c). This modest decrease in GP over the western portion of the WNP basin is due to a significant increase of TCCs which is partly cancelled out by a moderate increase in TCs.

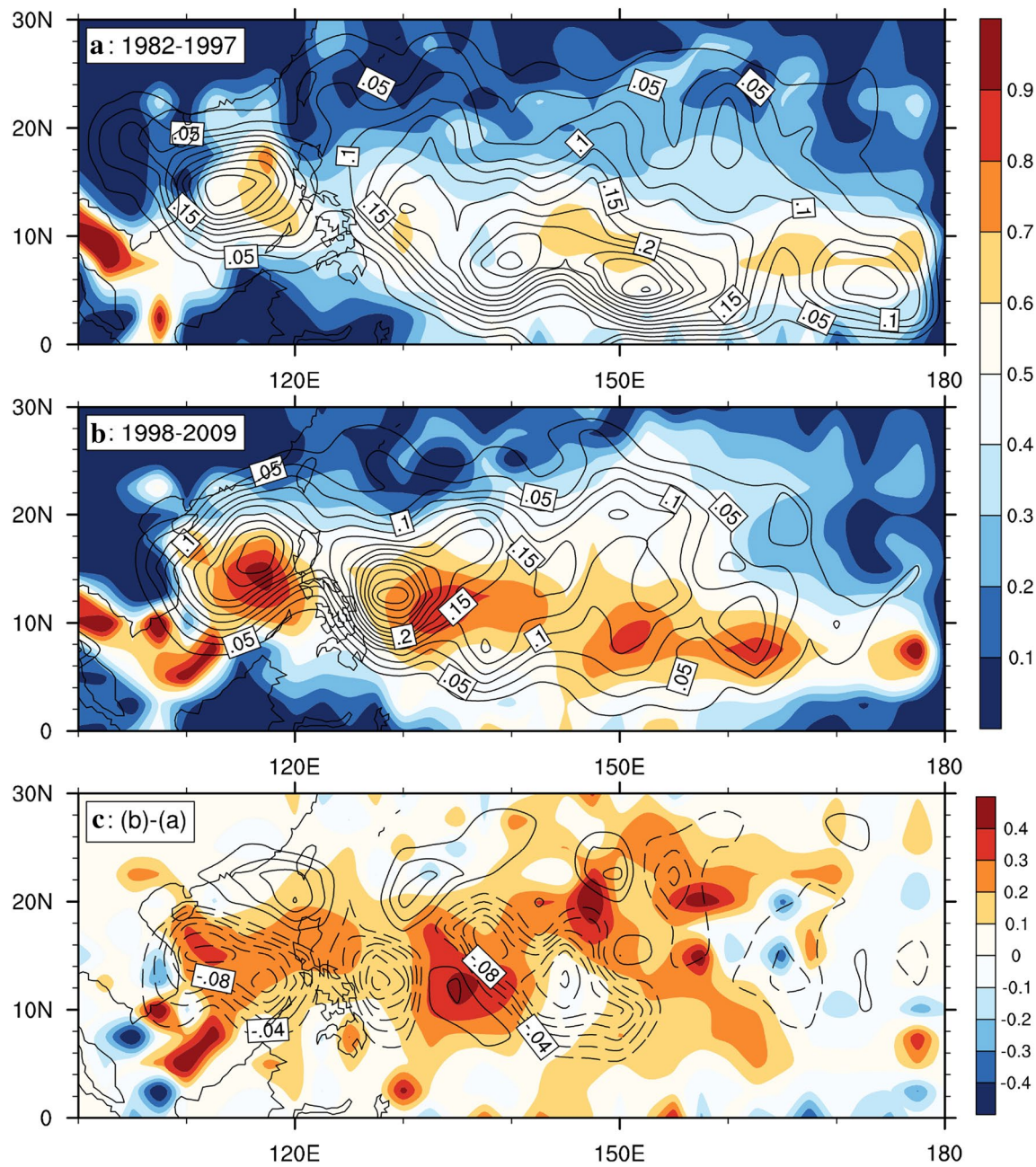


Fig. 2 Spatial distribution of boreal summer (July–October) tropical cloud clusters (TCCs) (shading) and tropical cyclones (TCs) (contour) over the WNP basin for the two sub-periods: **a** 1982–1997 and **b** 1998–2009, and their difference: **c** (1998–2009 minus 1982–1997)

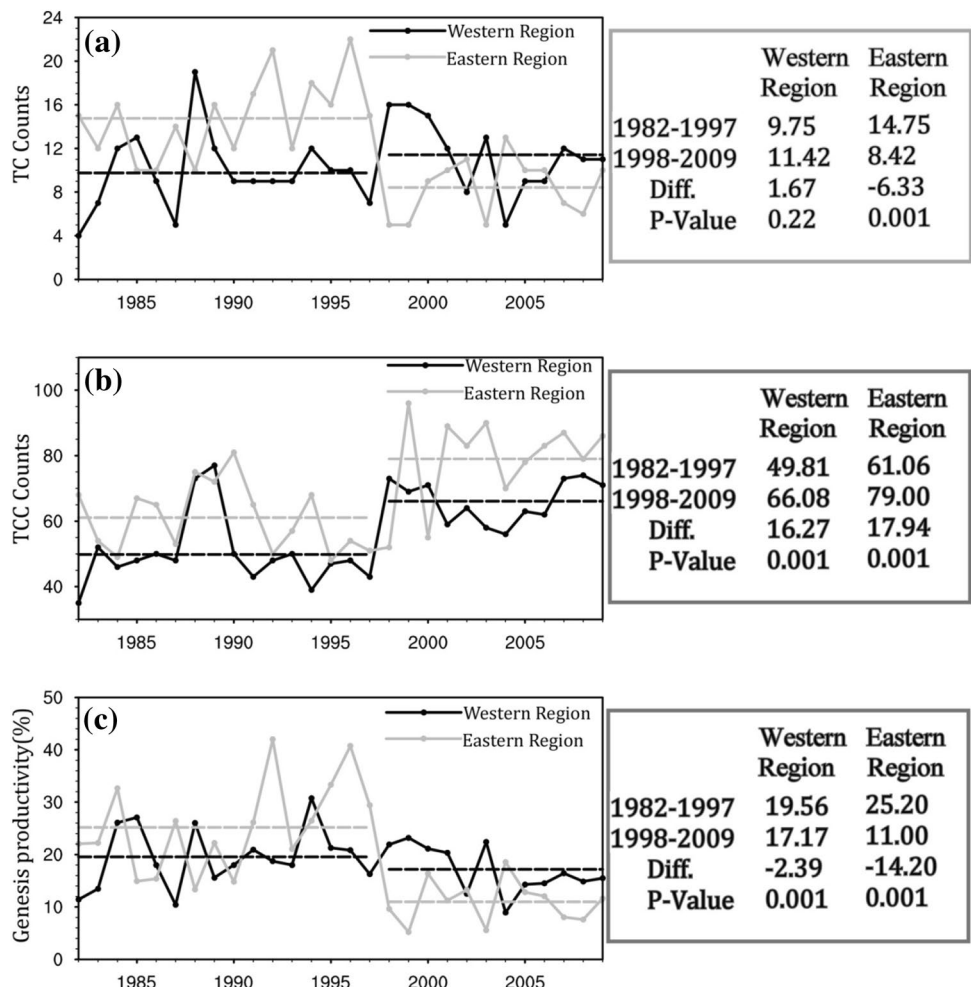
4 Changes in the large-scale environment

4.1 Spatiotemporal changes in large-scale factors associated with the recent decrease in GP

SST, 600 hPa relative humidity, 850 hPa relative vorticity and vertical wind shear are now compared between the two sub-periods before 1998 and since 1998 (Fig. 4). Over the whole WNP basin, significantly warmer SST are observed from 1998 to 2009 than were observed from 1982 to 1997

(Fig. 4a). Significant enhancements in mid-level moisture are also observed over most of the WNP during the recent decade, except for a significant decrease over the South China Sea (SCS) (Fig. 4b). These observed thermodynamic changes are conducive for enhancing both TCCs and TCs over the WNP basin. In contrast, a moderate decrease in 850 hPa relative vorticity is observed over the WNP basin during 1998–2009 (Fig. 4c), which would play a negative role in formation of both TCs and TCCs. The recent observed increase of vertical wind shear, especially over the eastern

Fig. 3 Time series of boreal summer (July–October) tropical cloud clusters (TCCs), tropical cyclones (TCs) and genesis productivity (GP) over the western region [0° – 30° N, 100° E– 140° E] and eastern region [0° – 30° N, 140° E– 180°] of the WNP basin during 1982–2009, and their corresponding average indicated by the dashed lines. The differences of averaged TCCs, TCs and TCCGP between the two sub-periods and the associated P-value are shown in the right box



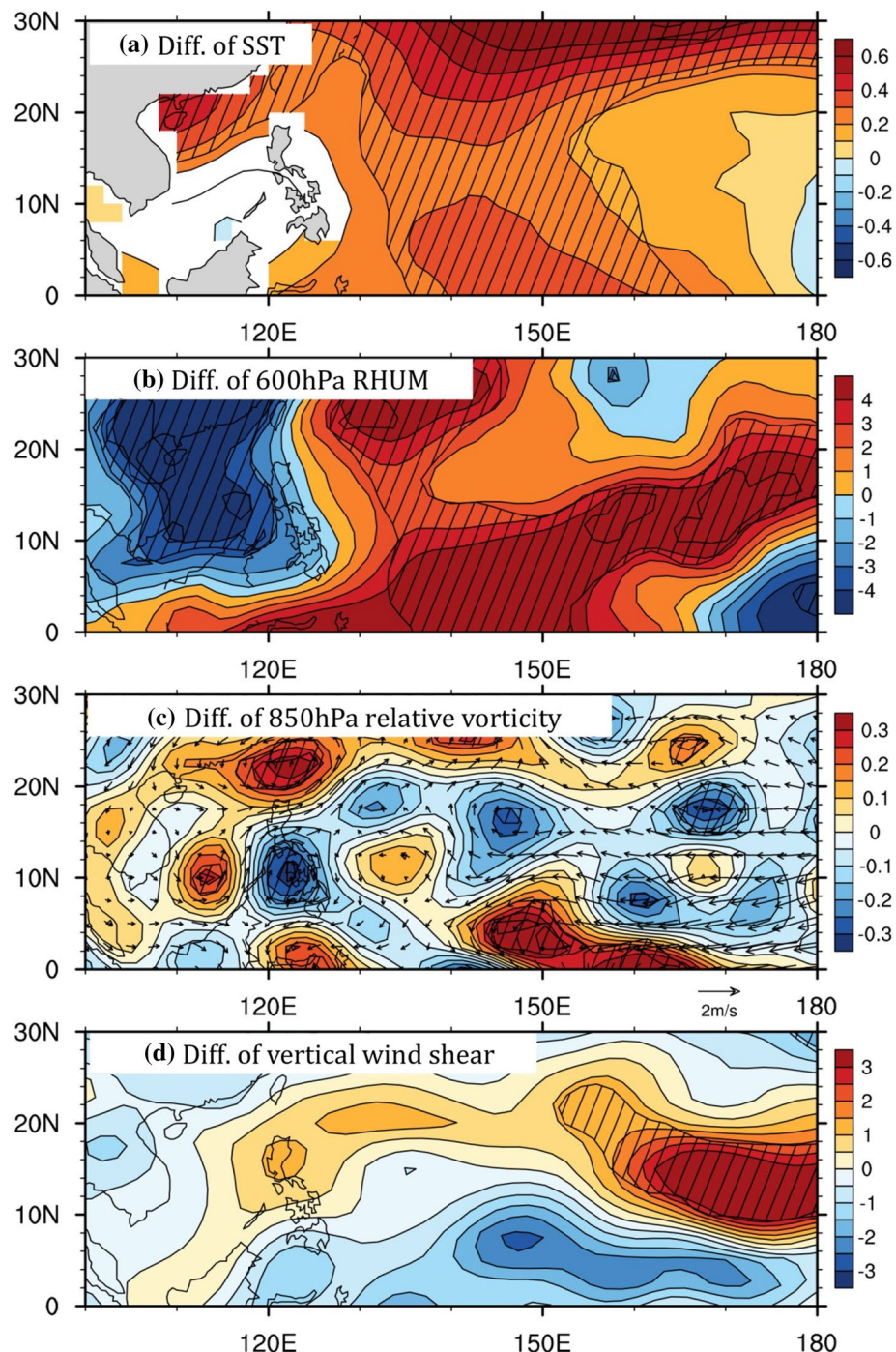
portion of the WNP basin (Fig. 4d), is favorable for the formation and development of TCCs but is unfavorable for TC genesis. This distinct role of vertical wind shear in TC genesis and TCC genesis has been noted in previous studies (Zehr 1992; Gray 1998; Kerns and Zipser 2009; Kerns and Chen 2013). To reinforce this observation, we compute the correlation between vertical wind shear and TCC and TC counts over the eastern portion of the WNP basin. As expected, a significant negative correlation of -0.58 is observed between TC count and vertical wind shear from 1982 to 2009 (Fig. 5a). In contrast, a positive correlation of 0.49 is observed between TCC count and vertical wind shear (Fig. 5b). These results imply that changes of vertical wind shear are likely one of the most important factors affecting TCC changes between the two sub-periods over the WNP basin. The underlying physical mechanism responsible for the development and genesis of TCCs merit a further study.

When large-scale factors are averaged over the whole WNP basin and compared between the two sub-periods, only SST experiences a significant increase since 1998, while the mid-level moisture, vertical wind shear, and low-level

vorticity have no significant change, as seen in Table 1. While mid-level moisture averaged over the whole WNP basin did not undergo a significant change, most of the WNP basin did experience a significant increase (Fig. 4b) which has been compensated in the basinwide average by a significant decrease over the SCS.

The analysis of the differences between the two sub-periods separating the WNP into a western and eastern region is shown in Table 2. Only the SSTs have significantly increased over both the eastern and western regions of WNP basin in the recent decades. The decreased low-level relative vorticity over the two sub-regions during the recent decades is not statistically significant. A small decrease in mid-level relative humidity is seen since 1998 over the western portion of the WNP basin, which is related to its significant decrease over the SCS (Fig. 4c). In contrast, mid-level moisture significantly increased over the eastern portion of the WNP basin during 1998–2009. The vertical wind shear over the eastern portion of the WNP has significantly increased over the recent decades, but the decrease over the western portion of the WNP leads to a small insignificant increase for the entire WNP basin. In

Fig. 4 Composite boreal summer (July–October) differences (1998–2009 minus 1982–1997) of the spatial distribution for sea surface temperatures (SST) (a), 600 hPa relative humidity (b), 850 hPa relative vorticity (c) and vertical wind shear (d). The diagonal line represents statistically significant at the 95% confidence level



summary, the recent decrease of GP over the WNP basin is the result of the combined spatiotemporal changes of the large-scale environment. The changes in thermodynamic factors during recent decades (e.g., increased SST and increased mid-level moisture) are favorable for TCC genesis over the WNP basin. Increased vertical wind shear over the eastern portion of the WNP basin has also aided in causing a significant increase of TCCs over the WNP basin during 1998–2009. These TCC-enhancing effects are partly offset by a moderate decrease of

850 hPa relative vorticity over the WNP basin as a whole and particularly by a significant decrease in the eastern region.

4.2 Relative importance of large-scale environmental factors contributing to the recent decrease in GP

Inter-decadal changes in large-scale environmental conditions are responsible for the observed changes in TCCs and

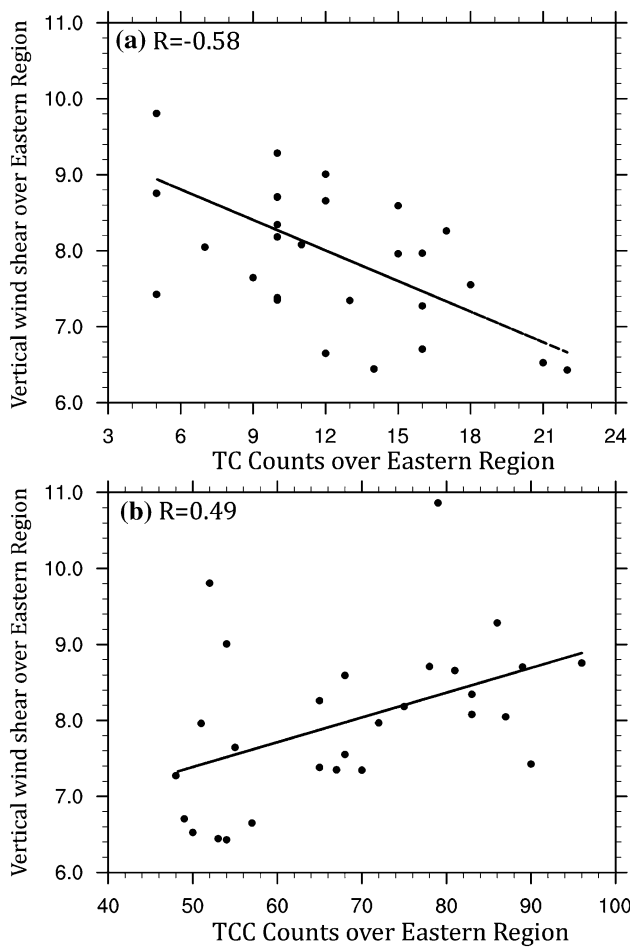


Fig. 5 Correlations of inter-annual boreal summer (July–October) (a) tropical cyclone (TC) counts and (b) tropical cloud cluster (TCC) counts of the western North Pacific basin with averaged vertical wind shear averaged over the eastern region [0°–30°N, 140°E–180°] during 1982–2009

TCs and consequently GP over the WNP basin. Using the GPI analyses following Camargo et al. (2007), the quantitative role of each of these large-scale factors in contributing to the recent decrease of GP over the WNP basin will now be assessed.

As shown in Fig. 6a, the observed differences in the GPI over the WNP basin correspond well to the observed differences in GP over the WNP basin between the two sub-periods. There is some inconsistency noted over the region from 0 to 10°N, 140°E–155°E. Nevertheless, there is good consistency between GP and GPI over the MDR of the WNP basin, indicating that the GPI has considerable skill in representing the changes of GP at least over the key region from 10°N–20°N, 100°E–180°. The separate role of each of the four factors included in the GPI is displayed in Fig. 6b–e. There is a negative GPI difference since 1998 with varying vertical wind shear (GPI-Shear), varying 850 hPa relative vorticity (GPI-VOR) and varying PI (GPI-PI) over the MDR of the WNP basin. In contrast, there is a positive GPI difference since 1998 with varying mid-level relative humidity (GPI-RH). These changes in spatial patterns together with the amplitude of GPI differences over the MDR of the WNP basin (figure not shown), indicate that vertical wind shear appears to be the most important driver in contributing to the recent decrease of GP, with secondary contributions from the increased SSTs and decreased low-level vorticity. It is worth noting that these drivers of the recent decrease in GP over the WNP are partly cancelled out by enhanced mid-level relative humidity during recent decades.

4.3 Possible explanation for changes in the environmental factors

Different tropical SST anomaly (SSTA) distributions can drive different atmospheric conditions in the WNP through both their direct as well as their remote impacts (Wang et al. 2000; Xie et al. 2009; Zhan et al. 2011; Zhang et al. 2007; Zhao et al. 2014; Hsu et al. 2014). In this study, the SST difference (1998–2009 minus 1982–1997) shows a “Mega-La-Nina-like” pattern (Fig. 7a), as suggested by Wang et al. (2013). Associated with the Mega-La-Niña-like decadal pattern, there is a corresponding change in lower- and upper-level winds and an associated increase in vertical wind shear especially over the eastern WNP basin due to the strengthening of the subtropical high and easterly

Table 1 Statistics of the magnitude of environmental factors: sea surface temperature (SST), 850 hPa relative vorticity, vertical wind shear and 600 hPa relative humidity, averaged over the whole WNP basin for the two sub-periods 1982–1997 and 1998–2009

	SST (unit: °C)	850 hPa-VOR (unit: 10^{-6}s^{-1})	Vertical wind shear (unit: m s^{-1})	600 hPa-RHUM (unit: %)
1982–1997	29.1	2.7	9.7	53.9
1998–2009	29.3	2.3	10.3	54.9
Difference	0.2	0.4	0.6	1.0
P-value	0.004	0.44	0.11	0.11

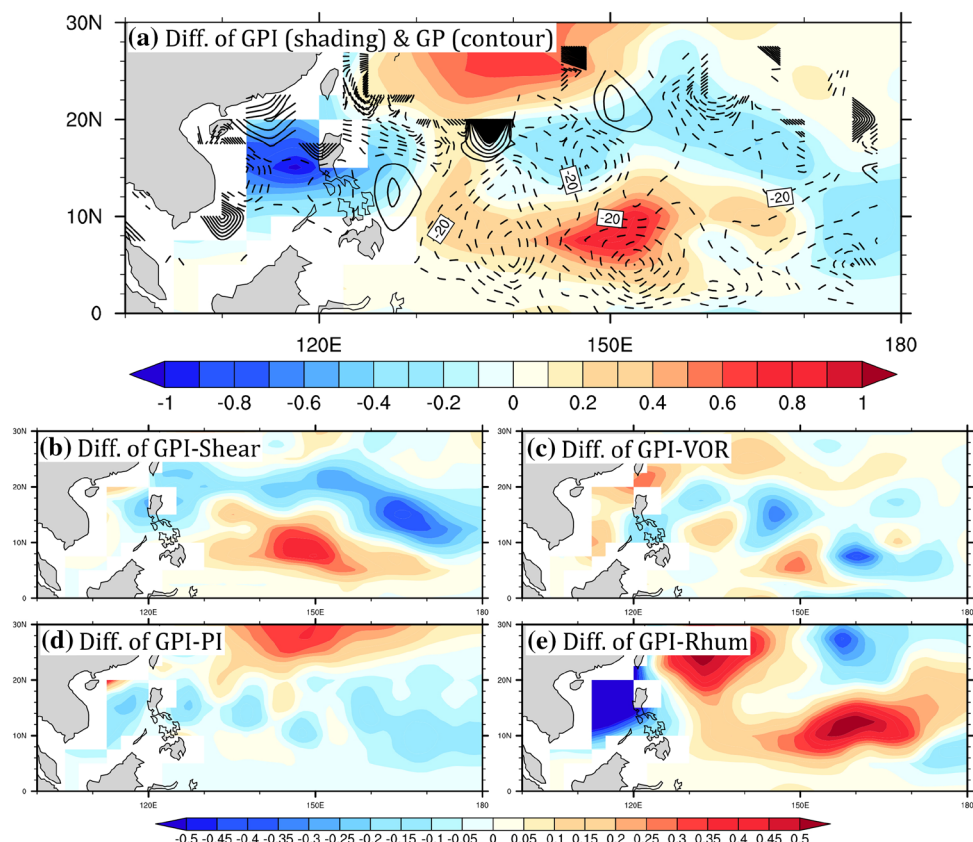
Their difference (1998–2009 minus 1982–1997) and the *p*-values are also listed. Differences that are significant at the 5% level are highlighted in bold

Table 2 Statistics of the magnitude of environmental factors: sea surface temperature (SST), 850 hPa relative vorticity, vertical wind shear and 600 hPa relative humidity, averaged over the western portion [0°–

30°N, 100°E–140°E] and eastern portion [0°–30°N, 140°E–180°] of the WNP basin for the two sub-periods 1982–1997 and 1998–2009

SST (unit: °C)		850hPa-VOR (unit: $10^{-6}s^{-1}$)		Vertical wind shear (unit: m s $^{-1}$)		600hPa-RHUM (unit: %)		
Western region	Eastern region	Western region	Eastern region	Western region	Eastern region	Western region	Eastern region	
1982–1997	29.1	29.1	3.3	2.1	11.8	7.6	59.3	48.4
1998–2009	29.3	29.2	3.3	1.4	11.8	8.6	58.3	51.6
Difference	0.2	0.1	0.0	−0.7	0.0	1.0	−1.0	3.2
P value	0.031	0.009	0.99	0.27	0.98	0.008	0.24	0.003

Fig. 6 **a** Difference (1998–2009 minus 1982–1997) of the averaged boreal summer (July–October) Genesis Potential Index varying all four variables (GPI-Total) and the difference of GP. Also displayed are the values of the difference in the GPI varying: **b** vertical wind shear (GPI-Shear), **c** 850 hPa relative vorticity (GPI-VOR) (d) potential intensity (GPI-PI) and **e** 600 hPa relative humidity (GPI-RH)

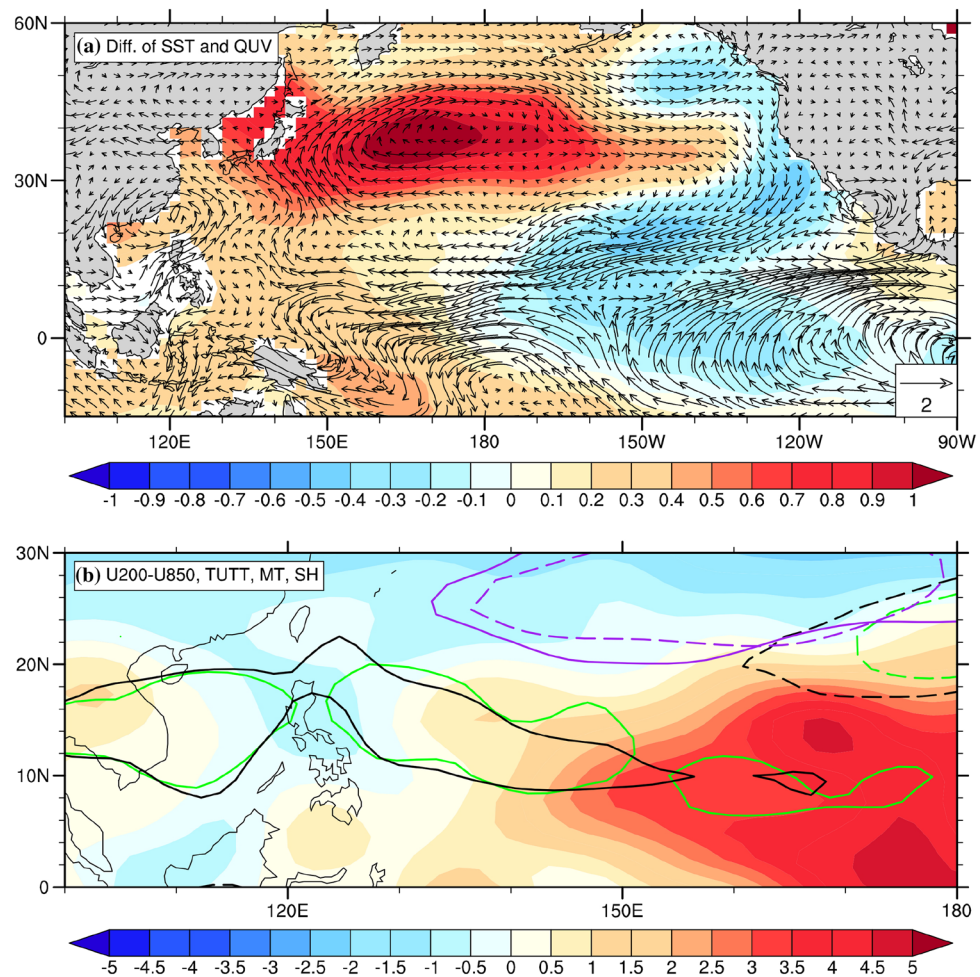


trade winds (Wang et al. 2013; Kosaka and Xie 2013; England et al. 2014; Lin and Chan 2015). These changes then enhance the moisture transport over the WNP basin (Fig. 7). As expected, the boreal summer low-level monsoon trough (MT) and the tropical upper tropospheric trough (TUTT), characterized by the large-scale environment over the WNP basin, show corresponding inter-decadal changes. Similar to Hu et al. (2018), the boreal summer (July–October) TUTT is identified by relative vorticity of $5 \times 10^{-6} s^{-1}$ at 200hPa, and the MT is identified by relative vorticity of $4 \times 10^{-6} s^{-1}$ at 850hPa. Observations indicate that there is a westward retreat of the MT and a westward shift of the TUTT over

the WNP basin during the recent decades (Fig. 7b). Following Wang and Wu (2016), we find that there has been a substantial westward shift of the TUTT cell and a northward expansion of the TUTT cell (figure not shown). These shifts result in decreased low-level vorticity and increased vertical wind shear, especially over the eastern portion of the WNP basin (Fig. 7b). Studies suggest that these circulation changes respond to changes in the global tropical SST pattern (Chan 2008; Wang et al. 2013, Hsu et al. 2014; Zhao and Wang 2016, 2018; Hu et al. 2018).

However, the underlying physical mechanism for the changes in the large-scale atmospheric patterns over the

Fig. 7 **a** Differences (1998–2009 minus 1982–1997) in boreal summer (July–October) vertically-integrated moisture flux (QUV, vector, $10^3 \text{ kg m}^{-1} \text{ s}^{-1}$). **b** Differences (1998–2009 minus 1982–1997) in boreal summer (July–October) zonal vertical wind shear between 200 and 850 hPa (shading, m s^{-1}). The boreal summer (July–October) TUTT is identified by relative vorticity of $5 \notin 10^{-6} \text{ s}^{-1}$ at 200 hPa for 1998–2009 (green dashed line) and 1982–1997 (black dashed line). The boreal summer (July–October) MT is identified by relative vorticity of $4 \notin 10^{-6} \text{ s}^{-1}$ at 200 hPa for the 1998–2009 (black solid line) and 1982–1997 (green solid line). The western North Pacific subtropical high (SH) is indicated by the purple solid line for 1998–2009 and the purple dashed line for 1982–1997. The western North Pacific subtropical high (SH) indicated by the 5870-gpm line of the 500 hPa geopotential height field is plotted by the purple solid line for 1998–2009 and the purple dashed line for 1982–1997



WNP basin remains unclear. Most recent studies have focused on the impact of changes of SST patterns in specific regions on circulation changes over other specific regions. For example, the recent significant decrease in the low-level circulation in the southeastern portion of the WNP basin has been mainly tied to anomalously warm SSTs in the tropical Indo-Pacific Ocean (Chan 2008; Hsu et al. 2014). Warm SST anomalies in the tropical Indian Ocean can enhance atmospheric anticyclonic anomalies to their east over the WNP basin by exciting a warm tropospheric equatorial Kelvin wave (Xie et al. 2009; Zhan et al. 2011; Tao et al. 2012). Other studies have shown that anomalous cooling in the eastern Pacific can play an important role in causing unfavorable conditions for TC genesis in the southeastern part of the WNP (Wang and Chan 2002; Camargo et al. 2005; Chan 2008; Zhao et al. 2011, 2014; Hsu et al. 2014; Hu et al. 2018). The impact of North Atlantic SST anomalies on changes in the large-scale environment affecting TC activity over the WNP basin have also been recently addressed (Hu et al. 2015; Yu et al. 2016; Gao et al. 2017).

While the importance of changes in regional SSTA in modulating the WNP circulations and the associated

large-scale factors has been explicitly indicated, the quantitative contributions of SSTA changes in different basins to the changes of the large-scale environment over the WNP basin should be further explored.

5 Summary

The significantly reduced TC frequency over the WNP basin since the late 1990s has been well documented in previous studies (Maue 2011; Liu and Chan 2013; Hu et al. 2014, 2018; Zhao and Wang 2016, 2018). While TCCs are typically referred to as precursors for TC genesis, studies on the variability of genesis productivity (GP, TCCs developing into TCs) at longer time scales remains limited. The longer-record of TCCs from 1982 to 2009 described in Hennon et al. (2011) provides a venue to further understand inter-decadal changes of GP over the WNP basin. In this study, we pose the question: how has the GP changed over the WNP basin in recent decades?

This study shows a significant decrease of GP over the WNP basin since 1998, coinciding with the abrupt decrease

of TC frequency over the WNP basin during recent decades. The recent decrease of GP over the WNP basin is further found to be mainly due to the significant decrease in GP over the eastern portion of the WNP basin from 1998 to 2009. Over the eastern portion of the WNP basin, significantly more TCCs and significantly fewer TCs are found. In contrast, no apparent change of GP over the western region of WNP basin is observed over the longer period (1982–2009). The positive role of the significant increase of TCCs in increasing GP over the western region of WNP basin is reduced by the moderate increase of TCs over this region.

The recent decrease of GP over the WNP basin is found to be closely associated with changes in the large-scale environment. Our analysis suggests that enhanced vertical wind shear is the most important factor for reducing GP over the WNP basin by enhancing TCCs and reducing TCs during the recent decades, especially over the eastern portion of the WNP basin. Secondary positive contributions to the recent decrease of GP over the WNP basin are found to be from increased SST and decreased low-level vorticity. These positive contributions to the reduced GP over the WNP basin during 1998–2009 are partly cancelled out by enhanced mid-level moisture. Changes of the large-scale environment appear to be closely associated with changes of the tropical SSTA pattern. In particular, the difference in SST (1998–2009 minus 1982–1997) shows a “Mega-La-Nina-like” decadal pattern. In response to such a Mega-La Nina-like pattern, there is an observed westward shift of the TUTT and a westward retreat of the MT over the WNP basin. This drives enhanced vertical wind shear and decreased low-level vorticity, especially over the eastern portion of the WP basin (Wang et al. 2013; Kosaka and Xie 2013; England et al. 2014; Lin and Chan 2015). However, the quantitative modulation of the large-scale atmospheric environment over the WNP due to changes in SSTs over various portions of the globe has yet to be fully assessed. These WNP atmospheric changes need to be examined not only considering regional impacts of SSTs but from an integrated global perspective examining SSTs in different basins.

As a final remark, in this study we performed an exploratory analysis of the inter-decadal changes of the relationship between TCCs and TCs over the WNP basin. As indicated by Hennon et al. (2013), the quality of the TCC data prior to 1998 may introduce some uncertainty in the results of this study. Therefore, we stress the need to test our observational results with more numerical simulations and additional observational analyses.

Acknowledgements This research was jointly supported by the National Natural Science Foundation of China (Grant nos. 41675072, 41730961 and 41475091), the Natural Science Foundation of Jiangsu Province (Grants No. BK20181412), the QingLan Project of Jiangsu Province (R2017Q01) and the Priority Academic Program

Development of Jiangsu Higher Education Institutions (PAPD). P. Klotzbach would like to acknowledge a grant from the G. Unger Vetlesen Foundation. The authors would like to thank the two anonymous reviewers for helpful comments that have significantly improved the manuscript.

References

- Bister M, Emanuel KA (2002) Low frequency variability of tropical cyclone potential intensity I. Interannual to interdecadal variability. *J Geophys Res* 107:4801. <https://doi.org/10.1029/2001JD000776>
- Camargo SJ, Sobel AH (2005) Western North Pacific tropical cyclone intensity and ENSO. *J Climate* 18:2996–3006. <https://doi.org/10.1175/JCLI3457.1>
- Camargo SJ, Emanuel KA, Sobel AH (2007) Use of a genesis potential index to diagnose ENSO effects on tropical cyclone genesis. *J Climate* 20:4819–4834. <https://doi.org/10.1175/JCLI4282.1>
- Camargo SJ, Wheeler MC, Sobel AH (2009) Diagnosis of the MJO modulation of tropical cyclogenesis using an empirical index. *J Atmos Sci* 66:3061–3074. <https://doi.org/10.1175/2009JAS3101.1>
- Chan JCL (2005) Interannual and interdecadal variations of tropical cyclone activity over the western North Pacific. *Meteor Atmos Phys* 89:143–152. <https://doi.org/10.1007/s00703-005-0126-y>
- Chan JCL (2008) Decadal variations of intense typhoon occurrence in the western North Pacific. *Proc Royal Soc A* 464:249–272
- Chen TC, Yen MC, Loon HV (1996) An observational study of the tropical-subtropical semiannual oscillation. *J Climate* 9:1993–2002
- Chen TC, Wang SY, Yen MC (2006) Interannual variation of the tropical cyclone activity over the Western North Pacific. *J Climate* 19:5709. <https://doi.org/10.1175/JCLI3934.1>
- Chen TC, Wang SY, Yen MC, Clark AJ (2008) Are tropical cyclones less effectively formed by easterly waves in the western North Pacific than in the North Atlantic? *Mon Wea Rev* 136:4527–4540
- Dee DP, Uppala SM, Simmons AJ (2011) The ERA-Interim reanalysis: configuration and performance of the data assimilation system. *Q J Roy Meteor Soc* 137:553–597. <https://doi.org/10.1002/qj.828>
- DeMaria M, Knaff JA, Connell BH (2001) A tropical cyclone genesis parameter for the tropical Atlantic. *Weather Forecast* 16:219–233
- Emanuel KA, Nolan DS (2004) Tropical cyclone activity and the global climate system. Preprints. In: 26th Conference on Hurricanes and Meteorology T, Miami, FL, Amer. Meteor. Soc., 240–241
- England MH et al (2014) Recent intensification of wind-driven circulation in the pacific and the ongoing warming hiatus. *Nat Clim Change* 4:222–227
- Fu B, Peng MS, Li T, Stevens DE (2010) Developing versus nondeveloping disturbances for tropical cyclone formation. Part II: Western North Pacific. *Mon Wea Rev* 140:1067–1080
- Gao S, Chen Z, Zhang W (2017) Impacts of tropical north Atlantic SST on western north pacific landfalling tropical cyclones. *J Climate* 31:853–862
- Garner ST, Held IM, Knutson T, Sirutis J (2009) The roles of wind shear and thermal stratification in past and projected changes of Atlantic tropical cyclone activity. *J Climate* 22:4723–4734. <https://doi.org/10.1175/2009JCLI2930.1>
- Goebbert KH, Leslie LM (2010) Interannual variability of northwest Australian tropical cyclones. *J Climate* 23:4538–4555. <https://doi.org/10.1175/2010JCLI3362.1>
- Gray WM (1968) Global view of the origin of tropical disturbances and storms. *Mon Wea Rev* 96:87
- Gray WM (1998) The formation of tropical cyclones. *Meteor Atmos Phys* 67:37–69. <https://doi.org/10.1007/BF01277501>

- Hennon CC, Hobgood JS (2003) Forecasting tropical cyclogenesis over the Atlantic basin using large-scale data. *Mon Wea Rev* 131:2927–2940
- Hennon CC, Marzban C, Hobgood JS (2005) Improving tropical cyclogenesis statistical model forecasts through the application of a neural network classifier. *Weather Forecast* 20:1073–1083
- Hennon CC, Helms CN, Knapp KR (2011) An objective algorithm for detecting and tracking tropical cloud clusters: implications for tropical cyclogenesis prediction. *J Atmos Ocean Tech* 28:1007–1018. <https://doi.org/10.1175/2010JTECHA1522.1>
- Hennon CC, Papin PP, Zarzar CM (2013) Tropical cloud cluster climatology, variability, and genesis productivity. *J Climate* 26:3046–3066. <https://doi.org/10.1175/JCLI-D-12-00387.1>
- Holland GJ (1995) Scale interaction in the western Pacific monsoon. *Meteorol Atmos Phys* 56:57–79
- Hsu PC, Chu P-S, Murakami H, Zhao X (2014) An abrupt decrease in the late-season typhoon activity over the western North Pacific. *J Climate* 27:4296–4312. <https://doi.org/10.1175/JCLI-D-13-00417.1>
- Hu W, Wu R, Liu Y (2014) Relation of the south China Sea precipitation variability to tropical Indo-Pacific SST anomalies during spring-to-summer transition. *J Climate* 27:5451–5467
- Hu C, Zhang C, Yang S, Chen D, He S (2018) Perspective on the northward shift of autumn tropical cyclogenesis locations over the western North Pacific from shifting ENSO. *Climate Dyn* 1–11
- Huang P, Chou C, Huang R (2011) Seasonal Modulation of Tropical Intraseasonal Oscillations on Tropical Cyclone Genes in the Western North Pacific. *J Climate* 24:6339–6352. <https://doi.org/10.1175/2011JCLI4200.1>
- Huo L, Guo P, Hameed SN, Jin D (2015) The role of tropical Atlantic SST anomalies in modulating western North Pacific tropical cyclone genesis. *Geophys Res Lett* 42:2378–2384. <https://doi.org/10.1002/2015GL063184>
- Jiang X (2012) Simulation of the intraseasonal variability over the Eastern Pacific ITCZ in climate models. *Climate Dyn* 39:617–636. <https://doi.org/10.1007/s00382-011-1098-x>
- Kanamitsu M, Coauthors (2002) NCEP–DOE AMIP-II reanalysis (r-2). *Bull Amer Meteor Soc* 83:1631–1643
- Kerns BW, Chen SS (2013) Cloud clusters and tropical cyclogenesis: developing and nondeveloping systems and their large-scale environment. *Mon Wea Rev* 141:192–210. <https://doi.org/10.1175/MWR-D-11-00239.1>
- Kerns B, Zipser E (2009) Four years of tropical ERA-40 vorticity maxima tracks. Part II: Differences between developing and nondeveloping disturbances. *Mon Wea Rev* 137:2576–2591
- Knapp KR, Kruk MC, Levinson DH, Diamond HJ, Neumann CJ (2010) The International Best Track Archive for Climate Stewardship (IBTrACS): Unifying tropical cyclone best track data. *Bull Amer Meteor Soc* 91:363–376. <https://doi.org/10.1175/2009BAMS27.55.1>
- Knapp KR et al (2011) Globally gridded satellite observations for climate studies. *Bull Am Meteor Soc* 92:893–907
- Kosaka Y, Xie SP (2013) Recent global-warming hiatus tied to equatorial Pacific surface cooling. *Nature* 501:403–407
- Lee CS, Edson R, Gray WM (1989) Some large-scale characteristics associated with tropical cyclone development in the North Indian Ocean during FGGE. *Mon Wea Rev* 117:407
- Lin LI, Chan JCL (2015) Recent decrease in typhoon destructive potential and global warming implications. *Nat Commun* 6:7182
- Liu KS, Chan JCL (2013) Inactive period of western North Pacific tropical cyclone activity in 1998–2011. *J Climate* 26:2614–2630. <https://doi.org/10.1175/JCLI-D-12-00053.1>
- Mapes BE, Houze RA (1993) Cloud clusters and superclusters over the oceanic warm pool. *Mon Weather Rev* 121:1398
- Maue RN (2011) Recent historically low global tropical cyclone activity. *Geophys Res Lett* 38:14803
- Mcbride JL, Zehr R (1981) Observational analysis of tropical cyclone formation. Part II: comparison of non-developing versus developing systems. *J Atmos Sci* 38:1132–1151
- Mohr KI, Zipser EJ (1996) Mesoscale convective systems defined by their 85-ghz ice scattering signature: size and intensity comparison over tropical oceans and continents. *Mon Wea Rev* 124:2417–2437
- Nesbitt SW, Zipser EJ, Cecil DJ (2000) A census of precipitation features in the tropics using TRMM: Radar, ice scattering, and lightning observations. *J Climate* 13:4087–4106
- Peng MS, Fu B, Li T, Stevens DE (2010) Developing versus non-developing disturbances for tropical cyclone formation. Part I: North Atlantic. *Mon Weather Rev* 140:1047–1066
- Perrone TJ, Lowe PR (1986) A statistically derived prediction procedure for tropical storm formation. *Mon Weather Rev* 114:165–177
- Smith TM, Reynolds RW, Peterson TC, Lawrimore J (2008) Improvements to NOAA's historical merged land–ocean surface temperature analysis (1880–2006). *J Climate* 21:2283–2296
- Tao L, Wu L, Wang Y (2012) Influence of tropical Indian ocean warming and ENSO on tropical cyclone activity over the western North Pacific. *J Meteorol Soc Jpn* 90:127–144
- Teng HF, Lee CS, Hsu HH (2014) Influence of ENSO on formation of tropical cloud clusters and their development into tropical cyclones in the western North Pacific. *Geophys Res Lett* 41:9120–9126. <https://doi.org/10.1002/2014GL061823>
- Tippett MK, Camargo SJ, Sobel AH (2011) A Poisson regression index for tropical cyclone genesis and the role of large-scale vorticity in genesis. *J Climate* 24:2335–2357. <https://doi.org/10.1175/2010JCLI3811.1>
- Wang B, Chan JCL (2002) How strong ENSO events affect tropical storm activity over the western North Pacific. *J Climate* 15:1643–1658
- Wang C, Wu L (2016) Interannual shift of the tropical upper-tropospheric trough and its influence on tropical cyclone formation over the western North Pacific. *J Clim* 29:4203–4211. <https://doi.org/10.1175/JCLI-D-15-0653.1>
- Wang B, Wu R, Fu X (2000) Pacific–East Asian teleconnection: how does ENSO affect East Asian climate? *J Climate* 13:1517–1536
- Wang C, Li C, Mu M, Duan W (2013) Seasonal modulations of different impacts of two types of ENSO events on tropical cyclone activity in the western North Pacific. *Climate Dyn* 40:2887–2902
- Williams M, Houze RA (1987) Satellite-observed characteristics of winter monsoon cloud clusters. *Mon Wea Rev* 115:505–519
- Wu L, Duan J (2014) Extended simulation of tropical cyclone formation in the western North Pacific monsoon trough. *J Atmos Sci* 72:150918123147005
- Wu L, Wang C, Wang B (2015a) Westward shift of western North Pacific tropical cyclogenesis. *Geophys Res Lett* 42:1537–1542
- Wu L, Wang C, Wang B (2015b) Westward shift of western North Pacific tropical cyclogenesis. *Geophys Res Lett* 42:1537–1542. <https://doi.org/10.1002/2015GL063450>
- Xie SP et al (2009) Indian Ocean capacitor effect on Indo-western Pacific climate during the summer following El Niño. *J Climate* 22:730–747
- Yu J, Li T, Tan Z, Zhu Z (2016) Effects of tropical North Atlantic SST on tropical cyclone genesis in the western North Pacific. *Climate Dyn* 46:865–877. <https://doi.org/10.1007/s00382-015-2618-x>
- Zehr RM (1992) Tropical Cyclogenesis in the Western North Pacific. Thesis—COLORADO STATE UNIVERSITY
- Zhan R, Wang Y, Wu CC (2011) Impact of SSTAs in the East Indian Ocean on the frequency of northwest Pacific tropical cyclones: a regional atmospheric model study. *J Climate* 24:6227–6242
- Zhang Y, Klein S, Mace GG, Boyle J (2007) Cluster analysis of tropical clouds using CloudSat data. *Geophys Res Lett* 34:195–225. <https://doi.org/10.1029/2007GL029336>

- Zhao H, Raga GB (2014) The influence of large-scale circulations on the extremely inactive tropical cyclone activity in 2010 over the western North Pacific. *Atmósfera* 27:353–365. [https://doi.org/10.1016/S0187-6236\(14\)70034-7](https://doi.org/10.1016/S0187-6236(14)70034-7)
- Zhao H, Wang C (2016) Interdecadal modulation on the relationship between ENSO and typhoon activity during the late season in the western north pacific. *Climate Dyn* 47:315–328
- Zhao H, Wang C (2018) On the relationship between ENSO and tropical cyclones in the western north pacific during the boreal summer. *Climate Dyn* 8:1–14
- Zhao H, Wu L (2017) Modulation of convectively coupled equatorial Rossby wave on the western North Pacific tropical cyclones activity. *Int J Climatol*. <https://doi.org/10.1002/joc.5220>
- Zhao H, Wu L, Zhou W (2011) Interannual changes of tropical cyclone intensity in the western North Pacific. *J Meteorol Soc Jpn* 89:243–253
- Zhao H, Chu P, Hsu P, Murakami H (2014) Exploratory analysis of extremely low tropical cyclone activity during the late-season of 2010 and 1998 over the western North Pacific and the South China Sea. *J Adv Model Earth Syst* 6:1141–1153
- Zhao H, Jiang X, Wu L (2015a) Modulation of Northwest Pacific tropical cyclone genesis by the intraseasonal variability. *J Meteor Soc Jpn* 91:81–97. <https://doi.org/10.2151/jmsj.2015-006>
- Zhao H, Yoshida R, Raga GB (2015b) Impact of the Madden-Julian Oscillation on Western North Pacific Tropical Cyclogenesis Associated with Large-scale Patterns. *J Appl Meteor Climatol* 54:1423–1429. <https://doi.org/10.1175/JAMC-D-14-0254.1>
- Zhao H, Jiang X, Wu L (2016) Boreal summer synoptic-scale waves over the western North Pacific in multi-model simulations. *J Climate*. <https://doi.org/10.1175/JCLI-D-15-0696.1>
- Zhao H, Raga GB, Klotzbach PJ (2017) Impact of the boreal summer quasi-biweekly oscillation on Eastern North Pacific tropical cyclone activity. *Int J Climatol* 656. <https://doi.org/10.1002/joc.5250>
- Zhao H, Duan X, Raga GB, Klotzbach PJ (2018) Changes in Characteristics of Rapidly Intensifying Western North Pacific Tropical Cyclones Related to Climate Regime Shifts. *J Climate*. <https://doi.org/10.1175/JCLI-D-18-0029.1>